

Facile Synthesis of ZnO Nanocomposite By An Alginate Mediated Process And A Case Study For Photocatalytic degradation of MB Dye

T. Uma Rajalakshmi^{1,2*} and G. Alagumuthu³

¹Research scholar (Reg.no. 12121) P.G & Research department of chemistry, Sri Paramakalyani College, Alwarkurichi-627 412. (Affiliated to Manonmaniam Sundaranar University, Tirunelveli-627 012, TN, India.)

²Department of chemistry, Rani Anna Govt. College for Women. Tirunelveli-627 008. Tamilnadu India. (Affiliated to Manonmaniam Sundaranar University, Tirunelveli-627 012, Tamilnadu, India.)

³Former Head, P.G & Research department of chemistry, Sri Paramakalyani College, Alwarkurichi-627 412. (Affiliated to Manonmaniam Sundaranar University, Tirunelveli-627 012, Tamilnadu, India.)

Abstract:

Nanostructured zincoxide can be synthesized by various methods such as physical, chemical, electrochemical, etc. but chemical route has attracted much attention due to the flexibility of controlling the shape and size of the structures by tuning the different growth conditions. In this work zincoxide nanoparticles are synthesized in the first stage followed by the synthesis of zincoxide/biopolymer nanocomposite in the second stage under suitable conditions. The synthesized zincoxide/biopolymer nanocomposite is characterized by the instrumental analysis viz XRD, SEM, TEM, FTIR etc. The XRD pattern showed the crystalline nature and the hexagonal structure of zincoxide. The shift and change in intensity of various stretching and bending FTIR modes shows the formation of the nanocomposite. The use of the nanocomposite as a photocatalyst was studied against methyleneblue dye.

Keywords: Nanocomposite, zincoxide, bio polymer, XRD, SEM, TEM.

1. Introduction:

Nano zincoxide (ZnO) attracted extensive research because of its characteristic features and novel applications in wide areas of science and technology. Zincoxide is a suitable alternative to TiO₂ because its photodegradation mechanism has been proven to be similar to that of TiO₂. In fact, in

comparison to TiO₂, zincoxide has been reported to have higher photocatalytic efficiency [1]. Zincoxide can absorb over a larger fraction of UV radiation, and the corresponding threshold of zincoxide is 425nm [2]. Zincoxide (ZnO) is a unique material with a direct band gap (3.34eV) and large excitation binding energy of 60meV [3,4]. It has been widely used in near UV emission, gas sensors, transparent conductor and piezoelectric applications [5-9]. Among the natural polymers, sodiumalginate is a natural linear polysaccharide consisting of mannuronic acid and guluronic acid units [10-16]. Alginate proved to have biocompatibility, non-toxicity, non-immunogenicity, biodegradability, antimicrobial activity, and can be simply gelled with divalent cations. Water pollution has become one of the major issues as it contains heavy ions and reactive dyes from industries. The wastes from the textile and dye industries are very poisonous, toxic and harmful for the living under water and human beings [17,18]. Many attempts have been made to overcome this problem. Lizama et al. reported zincoxide is more efficient catalyst than TiO₂ in degrading reactive blue 19 (RB-19) in aqueous solutions [19]. Zincoxide semiconductors with direct wide band gap are highly efficient n-type semiconductors having high electron-hole binding energy (60meV), and applications in photocatalysis have received a great deal of interest because of its good catalytic activity and quantum efficiency [20]. Various zincoxide nanostructures

have been used to degrade the harmful dyes by photocatalytic reaction under sunlight. We have utilized zinc oxide / biopolymer photocatalyst for the degradation of methylene blue dye. Methylene blue (MB) is a heterocyclic aromatic chemical compound used as a dye & as a pharmaceutical drug. It enters water bodies through effluents from textile, paper, and pharmaceutical industries and adversely affects eco-system and aquatic life. Presence of methylene blue in drinking water is a health hazard as it causes eye and skin irritation, hemolytic anemia, nausea, vomiting, and abdominal pain. Therefore, its removal from the polluted water is of significant importance. In the present work, a direct precipitation method was employed to synthesize nano-sized zinc oxide particles, followed by the formation of zinc oxide/biopolymer nanocomposite. The structural characteristics of the nanocomposite were determined by XRD, SEM, TEM, FTIR etc.

2. Experimental

Zinc nitrate, ammonium carbonate, sodium alginate and ethanol were available from Merck, India Pvt. Ltd. Deionised water was used throughout the reaction process. All the reagents used in this study were of analytical grade. The $Zn(NO_3)_2$ solution (1.5 mol/L) was slowly dropped into the $(NH_4)_2CO_3$ solution (2.25 mol/L) with vigorous stirring. And then, the precipitate derived from the above reaction was collected by filtration and rinsed three times with high-purity water followed by ethanol. Subsequently the washed precipitate was dried at 80 °C to form the precursor zinc oxide. Finally, the precursors were calcined at a temperature of 550 °C for 2 hr in the muffle furnace [21] to obtain the nano-sized zinc oxide particles. The precursor zinc oxide nanoparticles were mixed with 100 ml of a solution containing biopolymer sodium alginate under proper proportions and stirred uniformly for about 6 hours. The resulting mixture was poured in an autoclave coated with teflon lining maintained at 180 °C for 12 hours, filtered, washed with ethanol and water and dried at 80 °C for 2 hours. The synthesized nanocomposite was characterized by XRD, SEM, TEM, FTIR, etc. Photocatalytic degradation was carried out using the synthesized nanocomposite against MB dye.

3. Characterisation techniques

X-ray diffraction (XRD) studies were carried out for the synthesized nanocomposites using a Philips powder X-ray diffractometer (Model: PW1710). The XRD patterns were recorded in the 2θ range of 10° - 80° with step width 0.02° and step time 1.25 sec using $CuK\alpha$ radiation ($\lambda = 1.5406 \text{ \AA}$). The XRD patterns were analyzed by matching the observed peaks with the standard pattern provided

by JCPDS file. Fourier Transform Infra Red (FTIR) spectroscopy (Model: Perkin Elmer 100) of the nanocomposite was studied in the frequency range of 400 - 4000 cm^{-1} . Morphological study of nanocomposite was carried out using scanning electron microscopy (SEM Model: JEOL JSM 6360) at 20 kV. HRTEM was performed for the nanocomposites using a JEOL JEM-3100F transmission electron microscope.

4. Results and discussion

4.1 XRD

X-ray diffraction pattern is used to confirm the purity, phase, average particle size and overall crystallinity of the synthesized nanocomposites. From Fig. 4.1, the peaks at $2\theta = 31^\circ, 34^\circ, 36^\circ, 47^\circ, 56^\circ, 62^\circ, 67^\circ$ and 69° of zinc oxide/sodium alginate nanocomposites are corresponding to (100), (002), (101), (102), (110), (103), (112) and (201) in the JCPDS data card 89-0510. Hexagonal structure of zinc oxide was confirmed by the (1 0 1) crystalline peak and the average crystal size of synthesized nanoparticle is in the range 39-41 nm. The presence of sodium alginate as well as characteristic reflections indicated the maintenance of the sodium alginate and zinc oxide nanoparticles in crystallographic organization of the nanocomposites. The presence of high and narrow shaped peaks highlights that zinc oxide nanoparticles possess high crystallinity and low surface defects and were of ultrapure phase.

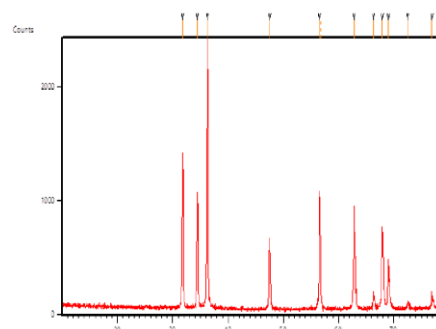


Fig.4.1 XRD pattern of zinc oxide/sodium alginate nanocomposite

4.2 SEM

Figure 4.2 depicts the uniform distribution of granular zinc oxide into the polymer matrix. It is observed that zinc oxide particles are almost spherical in shape, surrounded by the polymer matrix & hence it appears as agglomerated macromolecules.

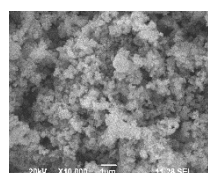


Figure 4.2 Shows the SEM image of the synthesised zincoxide /sodiumalginate nanocomposite

4.3 TEM

Figure 4.3 shows the TEM image of the prepared zincoxide /sodiumalginate nanocomposite. The size of the particle observed is in the range of 40-45nm which is in good agreement with Debye-Scherer formula using XRD. After composite formation, zincoxide nanoparticles were found to be entrapped in the bio polymer matrix.

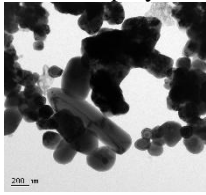


Figure 4.3 Shows the TEM image of the prepared zincoxide /sodiumalginate nanocomposite

4.4 FTIR

Fourier transform infrared spectroscopy (FTIR) data of the zincoxide/sodiumalginate nanocomposite is represented in the figure 4.4. The absorption band characteristics of alginate were observed at 3448cm^{-1} corresponding to OH group and the peaks near 1637cm^{-1} , 1543cm^{-1} and 1460cm^{-1} are assigned to symmetric and asymmetric stretching vibration of COO^- groups (dang et al.,2018). The band around 1100cm^{-1} (C-O-C) stretching were attributed to its saccharide structure (nguyen et al.,2015). The absorption band around 2922cm^{-1} may be due to the C-H stretching of the CH_2 group. The peak around 450cm^{-1} is the characteristic absorption of Zn-O bond.

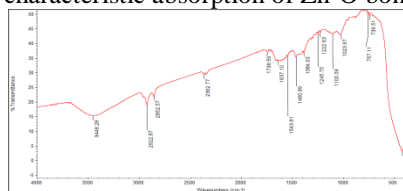


Figure 4.4 Shows the FTIR image of the zincoxide /sodiumalginate nanocomposite

4.5. UV-VIS absorption spectra

The room temperature UV-vis absorption spectra of zincoxide/biopolymer nanocomposite are shown in Fig4.5. The zincoxide/biopolymer nanocomposite was dispersed in ethanol with concentration of 0.1% wt and then the solution was used to perform the UV-vis measurement. The spectrum reveals a characteristic absorption peak of zincoxide at wavelength of 370 nm which can be assigned to the intrinsic band-gap absorption of zincoxide due to the electron transitions from the valence band to the conduction band ($\text{O}_{2p} \rightarrow \text{Zn}_{3d}$). In addition, this sharp peak shows that the

particles are in nanosize, and the particle size distribution is narrow.

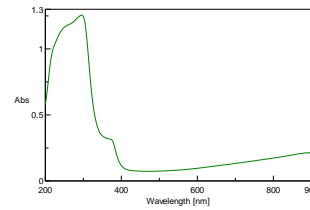


Fig4.5. UV-Vis absorption spectra of the synthesized nanocomposite.

4.6 AFM

Surface topology of the synthesized zincoxide nanoparticles was studied by Atomic Force microscope (AFM) analysis as shown in Fig.4.6 The results showed a uniform surface and indicated that the particles have uniform dimensions.

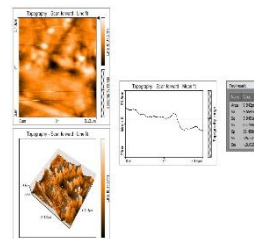


Figure 4.6 Shows the AFM image of the zincoxide /sodiumalginate nanocomposite

4.7 Photocatalytic degradation studies

4.7. (a). Effect of catalyst loading

The percentage of removal was found to enhance linearly with increase in the dose of the catalyst (2-12mg) indicating the heterogeneous regime. This may probably be due to: (i) increase in the extent of dye adsorption molecules on the catalyst surface; (ii) increase in the number of surface active sites; (iii) enhanced generation of hydroxyl radicals due to increase in the concentration of charge carriers [22-26].

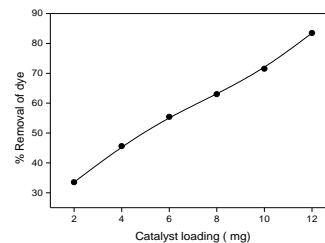
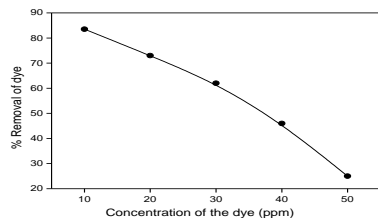


Fig4.7.(a). Variation of % removal of the dye against catalyst loading.

4.7.(b).Effect of initial concentration of dye

The initial concentration of the MB dye with constant catalytic loading (12mg/50ml) was varied from 10ppm to 50ppm. It was observed that the rate constant decreases from 10ppm to 50ppm dye concentration. This is due to the fact that more dye

molecules are available in the photoactive volume for the degradation process. Rate constant decreases with further increase in concentration of dye above the optimal value. The decrease is attributed to fact that the dye itself will start acting as a filter for the incident irradiation, reducing the photoactive volume. At low concentration, the reverse effect is observed [27] as shown in Fig.4.7.(b).



4.7.(b) Variation of % removal of the dye against concentration of the dye

4.7.(c).Effect of irradiation time

Irradiation time plays an important role in the photocatalytic degradation process of MB dye. Effect of irradiation time with constant dose of the catalysts (12mg/50 mL) and initial concentration (10ppm) of MB dye. It has been observed from the Fig.4.7.(c), that the percentage of photodegradation increases with increase in irradiation time and complete degradation was obtained with 150 minutes. This may be due to with increase in irradiation time dye molecules and catalysts have enough time to take part in photocatalytic degradation process and hence percentage of degradation increases [28]. The results of experiments showed that the photocatalytic degradation of MB dye obey apparently pseudo first order kinetics and the rate expression is given by the following equation,

$$\ln (C_0/C_t) = kt \text{ ----- (1)}$$

Where,

C_0 = initial concentration of dye solution

C_t = final concentration of dye solution

in various time interval

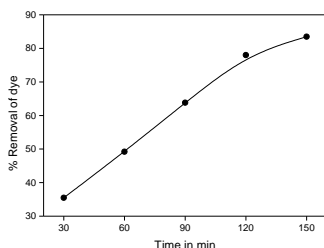


Fig4.7.(c) Variation of % removal of dye against irradiation time

4.7. (d) Effect of pH variation

The wastewater from textile industries usually has a wide range of pH values. Further, the generation

of hydroxyl radicals is also a function of pH. The pH is varied from 2 to 12 and the % removal of dye is noted. Higher percentage (73%, and 82%) removal occurred because at this basic condition the surface of the catalyst will become negatively charged so the cationic dye (MB) was easily attracted by the catalyst. So higher percentage removal occur in basic condition.

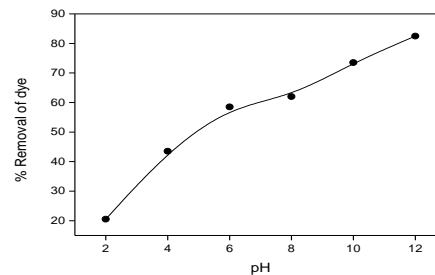


Fig.4.7.(d) Variation of % removal of dye against pH

4.7. (e) Reuse of Catalyst

The reuse of a 12 mg of synthesized biopolymer nanocomposite performed on a 10 ppm MB solution (50 mL) is expressed as the number of cycles, where the photocatalytic degradation of the nanocomposite was reduced from 85% on the first usage to 75%, 70% and 60% after the second, third and fourth cycles of reuse, respectively. This reduced dye photodegradation activity is in accord with the appearance of synthesized zincoxide biopolymer nanocomposite, which was clearly changed in the morphology of the synthesized zincoxide biopolymer nanocomposites due to the Photodegradation.

5. Conclusion

The zincoxide /sodiumalginate nanocomposite was prepared by a facile process. The XRD pattern of the synthesized nanocomposite shows that the size was approximately 40nm. From SEM analysis, it is found that the particles are almost spherical in shape in which the zincoxide nanoparticles were homogeneously dispersed in the biopolymer matrix. TEM results confirm that the zincoxide nano particles (with a mean diameter of (40-45nm) were encapsulated by the biopolymer. The FTIR spectra confirms the functional groups of alignate and zincoxide. UV-Vis absorbtion spectra reveals the characteristic absorbtion of zincoxide nanoparticles at 370 nm. Photocatalytic activity studies where performed effectively on MB dye and 82% removal was achieved at an optimum pH of 12 with catalytic loading of 12 mg in a dye concentration of 10 ppm.

References

- [1] Dindar, S & Icli, J. Unusual photoreactivity of zinc oxide irradiated by concentrated sunlight. *J. Photochem. Photobiol. A: Chem.* 140, 263–268 (2001)
- [2] Behnajady, M.A., Modirshahla, N., & Hamzavi, R: Kinetic study on photocatalytic degradation of C.I. Acid Yellow 23 by ZnO photocatalyst. *J. Hazard. Mater.* B133, 226–232 (2006).
- [3] Gyu-Chul Y, Chunrui W. and Won Il P. “ZnO nanorods: synthesis, characterization and applications” *Semicond. Sci. Technol*, 20, S22, (2005)
- [4] Qiuxiang Z, Ke Y, Wei B, Qingyan W, Feng X, Ziqiang Z, Ning D, & Yan S, “Synthesis, optical and field emission properties of three different ZnO nanostructures”, *Materials Letters*, 61, 3890, (2007)
- [5] Yuzhen L, Lin G, Huibin X, Lu D, Chunlei Y, Jiannong W, Weikun G, Shihe Y and Ziyu W, “Low temperature synthesis and optical properties of small-diameter ZnO nanorods”, *J. Appl. Phys.* 99, 114, 302, (2006)
- [6] Hachigo A, Nakahata H, Higaki K, Fujii S and Shikata S-I, “Heteroepitaxial growth of ZnO films on diamond (111) plane by magnetron sputtering”, *Appl. Phys. Lett.* 65, 2556, (1994)
- [7] Morkoc H, Strite S, Gao G B, Lin M E, and Sverdlov B, and M. Burns, “Large-band-gap SiC, III-V nitride, and II-VI ZnSe-based semiconductor device technologies”, *J. Appl. Phys.* 76, 1363, (1994)
- [8] Spanhel L and Anderson M A, “Semiconductor Clusters in the Sol-Gel Process: Quantized Aggregation, Gelation, and Crystal Growth in Concentrated ZnO Colloids”, *J. Am. Chem. Soc.* 113, 2826, (1991)
- [9] Bagnall D M, Chen Y F, Shen M Y, Zhu Z, Goto T and Yao T, “Room temperature excitonic stimulated emission from zinc oxide epilayers grown by plasma-assisted MBE”, *J. Cryst. Growth*, 184/185, 605, (1998)
- [10] Paul W, Sharma CP. Chitosan and alginate wound dressings: A short review. *Trends Biomater Artif Organs*; 18(1):18–23. (2004)
- [11] Gu Z, Xie H, Huang C, Li L and Yu X. Preparation of chitosan/silk fibroin blending membrane fixed with alginate dialdehyde for wound dressing. *Int J Biol Macromol.*; 58:121–126, (2013).
- [12] Sarker B, Singh R, Silva R, et al. Evaluation of fibroblasts adhesion and proliferation on alginate-gelatin crosslinked hydrogel. *PLoS One.*; 9(9):e107952. (2014)
- [13] Pereira R, Carvalho A, Vaz DC, et al. Development of novel alginate based hydrogel films for wound healing applications. *Int J Biol Macromol.*; 52:221–230(2013).
- [14] Thu HE, Zulfakar MH, Ng SF. Alginate based bilayer hydrocolloid films as potential slow-release modern wound dressing. *Int J Pharm.* 2012; 434(1–2):375–383.
- [15] Goh CH, Heng PW, Huang EP, Li BK and Chan LW. Interactions of antimicrobial compounds with cross-linking agents of alginate dressings. *J Antimicrob Chemother.*; 62(1):105–118(2008).
- [16] Shalumon KT, Anulekha KH, Nair SV, et al. Sodium alginate/poly(vinyl alcohol)/nano ZnO composite nanofibers for antibacterial wound dressings. *Int J Biol Macromol.*; 49(3):247–254.
- [17] McCann, J., Ames, Proc Natl B.N Acad Sci USA 73(1976)959(2011).
- [18] Baldez. E.E., Robaina N.F, and Cassella, J Haz Mat R.J, 159, 580(2008)
- [19] C. Lizma, J. Freer, J. Baeza, H.D and Mansilla, *Catal. Today* 76, 235(2002).
- [20] Roy, S., Basu, *Bull S Mat Sci*, 25, 6(2002)
- [21] Chang chun chen, Ping Liu Chun Hua Lu Synthesis and characterization of nano-size ZnO powders by direct precipitation method *July* (2008)
- [22] Teoh W.Y., Scott J.A., Amal R., Progress in heterogeneous photocatalysis: from classical radical chemistry to engineering nanomaterials and solar reactors. *J. Phys. Chem. Lett.*, 3, 629, (2012)
- [23] Konstantinou, K and Albanis .T.A, TiO₂-assisted photocatalytic degradation of azo dyes in aqueous solution: kinetic and mechanistic investigations: A review. *Appl. Catal. B: Environ.*, 49, 1, (2004).
- [24] Baran, W., Makowski .A, Wardas, W, The effect of UV radiation absorption of cationic and anionic dye solutions on their photocatalytic degradation in the presence of TiO₂. *Dyes and Pigments.*, 76, 226, (2008)
- [25] R. Pasricha, S. Gupta, A.K. Srivastava, A facile and novel synthesis of Ag-graphene-nanocomposites. *Small.*, 5, 2253, (2009).
- [26] Neppolian, B, Choi. H.C, Sakthivel, S, Arabindoo, Band Murugesan, V, Solar/UV-induced photocatalytic degradation of three commercial textile dyes. *J. Hazard. Mater.* 89, 303(2002).
- [27] Kudo, A and Miseki, P Heterogeneous photocatalyst materials for water splitting. *Chem. Soc. Rev.* 38(2009), 253.
- [28] Meenakshi Sundaram M. Sangareswari and Mand Muthirulan, P Enhanced photocatalytic activity of polypyrrole/TiO₂ nanocomposites for acid violet dye degradation under UV irradiation, *Int. J. Innov. Res. Sci. Eng.* 2 420–423, (2014)